Oxidative potential in rural, suburban and city centre atmospheric environments in Central Europe

Máté VÖRÖSMARTY[1], Gaëlle UZU[2], Jean-Luc JAFFREZO[2], Pamela DOMINUTTI[2], Zsófia KERTÉSZ[3], Enikő PAPP[3], and Imre SALMA[4]

[1] Hevesy György Ph. D. School of Chemistry, Eötvös Loránd University, Budapest, Hungary
[2]University of Grenoble Alps, IRD, CNRS, INRAE, Grenoble, France
[3] Laboratory for Heritage Science, Institute for Nuclear Research, Debrecen, Hungary
[4] Institute of Chemistry, Eötvös Loránd University, Budapest, Hungary

Correspondence to: Imre Salma (salma.imre@ttk.elte.hu)

Abstract. Oxidative potential (OP) is an emerging health-related metric which integrates several physicochemical properties of particulate matter (PM) that are involved in the pathogenesis of the diseases resulting from the exposure to PM. Daily $PM_{2.5}$-fraction aerosol samples collected in the rural background of the Carpathian Basin and in the suburban area and centre of its largest city of Budapest in each season over one year were utilised to study the OP at the related locations for the first time. The samples were analysed for particulate matter mass, main carbonaceous species, levoglucosan and 20 chemical elements. The resulted data sets were subjected to positive matrix factorisation to derive the main aerosol sources. Biomass burning (BB), suspended dust, road traffic, oil combustion, vehicle metal wear and mixed industrial source were identified. The OP of the sample extracts in simulated lung fluid was determined by ascorbic acid (AA) and dithiothreitol (DTT) assays. The comparison of the OP data sets revealed some differences in the sensitivities of the assays. In the heating period, both the OP and PM mass levels were higher than in spring and summer, but there was a clear misalignment between them. In addition, the heating period-to-non-heating period OP ratios in the urban locations were larger than for the rural background by factors of 2–4. The OP data sets were attributed to the main aerosol sources using multiple linear regression with the weighted least squares approach. The OP was unambiguously dominated by BB at all sampling locations in winter and autumn. The joint effects of motor vehicles involving the road traffic and vehicle metal wear played the most important role in summer and spring, with considerable contributions from oil combustion and resuspended dust. In winter, there is temporal coincidence between the most severe daily PM health limit exceedances in the whole Carpathian Basin and the chemical PM composition causing larger OP. Similarly, in spring and summer, there is a spatial coincidence in Budapest between the urban hotpots of OP-active aerosol constituents from traffic and the high population density in central quarters. These features offer possibilities for more efficient season-specific air quality regulations focusing on well-selected aerosol sources or experimentally determined OP rather than on PM mass in general.

1 Introduction and objectives

Poor air quality caused by high concentrations of particulate matter (PM) is one of the most severe public health concerns for humans worldwide (e.g. Lelieveld et al., 2015, 2020; Bondy, 2016; Cohen et al., 2017). Its acute and chronic effects, such as lung, cardiovascular and cerebrovascular diseases have been documented in both epidemiological and toxicological studies (e.g. Donaldson et al., 2005; Valavanidis et al., 2008; Apte et al., 2015; Riediker et al., 2019; Kelly and Fussell, 2020).

Due to the chemical, physical and biological complexity of ambient aerosol particles, their dynamic character and possible synergisms among air pollutants, a sophisticated interplay of multiple factors is involved in the pathogenesis of the diseases resulting from the exposure to PM. The main factors can involve: 1) mass concentrations of $PM_{2.5}$ or PM_{10} size fractions, 2) amounts of potentially toxic chemical components such as transition and heavy metals, polycyclic aromatic hydrocarbons (PAHs), soot and specific organics, 3) certain chemical speciation forms such as Cr(VI) versus Cr(III), 4) lung bioaccessibility of critical constituents, 5) surface reactivity of particles, 6) number concentrations of very small particles such as ultrafine particles or engineered nanomaterials, 7) shape and morphology of particles such as for asbestos or silica and 8) active components of biogenic origin such as bacteria, viruses, pollens and moulds or with radioactivity such as radon progeny (Riediker et al., 2019). Therefore, it cannot be expected that a single or a few aerosol metrics broadly express the induced biological responses. In the first approximation, PM mass is often selected from these factors as a simplistic metric, and it can be refined by further particle properties.

One of the most important biological mechanisms by which PM induces adverse health effects is causing an oxidant-antioxidant imbalance in the respiratory system at the cellular level (Kelly and Mudway, 2003; Borm et al., 2007; Kelly and Fussel, 2012, 2015; Cassee et al., 2013; Valavanidis et al., 2013; Janssen et al., 2014). This is called as oxidative stress. It is related to 1) stimulating cells to uncontrolled production of excess reactive oxygen species (ROS) endogenously, e.g. directly by Fenton-type reactions of redox-active aerosol components in the human body or indirectly through biotransformation, e.g. of PAHs or 2) inefficient elimination of ROS by the antioxidant defence system of the body. These can lead to inflammatory processes that increase the risk for various diseases and can result in biological aging and apoptosis (Ayres et al., 2008; Verma et al., 2012; Gao et al., 2020). The capacity of PM to invoke oxidative stress is quantified by its oxidative potential (OP). This integrates several factors of the particle properties 1–8 listed above. Numerous epidemiological studies suggest that the OP can be one of the central quantities that is responsible for several health enpoints including specific acute effects such as emergency

treatment of asthma and congestive heart failure and that largely explains the underlying biological bases of toxicity (e.g. Bates et al., 2015; Kelly and Fussel, 2015; Abrams et al., 2017; Yue et al., 2018; Weichenthal et al., 2019; Daellenbach et al., 2020; Dhalla et al., 2000; Zhang et al., 2022; Baumann et al., 2023).

As a result, there has been a substantial and increasing scientific interest in the measurement improvements of OP using (biological) in vivo, in vitro cellular and in vitro acellular assays, and in the identification of the aerosol components and sources closely related to OP (e.g. Cho et al., 2005; Künzli et al., 2006; Boogaard et al., 2012; Verma et al., 2014, 2015; Kelly and Fussel, 2015; Fang et al., 2016; Calas et al., 2017; Weber et al., 2018; Shahpoury et al., 2021; Borlaza et al., 2021b, 2022; Lionetto et al., 2021; Zhang et al., 2022). The OP is frequently measured by acellular assays for exogenous ROS, in which the PM extract or the particles directly cause a consumption rate of some antioxidants such as ascorbic acid (AA) or of some chemical surrogates to cellular reducing agents, e.g. dithiothreitol (DTT). The quantifications are generally based on spectrophotometry. More sophisticated detection methods which directly determine the ROS production are also available (Katerji et al., 2019).

The most frequently used assays were compared for PM_{10}-fraction aerosol samples considering the chemical composition of particles as well (Calas et al., 2018; Lionetto et al., 2021; Shahpoury et al., 2022). It was concluded that the assays correlated with each other but were not equivalent. All assays were somewhat specific, and no consensus has been reached on the “best assay” nor on a standardised methodology for each assay (Weber et al., 2021; Zhang et al., 2022). At the same time, it seems sensible to compare the results obtained by an identical sample preparation and OP measurement method for different environmental types. Likewise, comparing the data derived by different experimental methods applied to similar sample types can contribute to revealing and understanding the different properties or characteristics of these methods for various chemical components and sources. Both approaches can also yield considerable methodological development.

The main common features of the assays are that 1) they exhibit different responses to various groups of ROS-generating compounds and their bioavailability, 2) their sensitivity depends on the partner reaction compound to ROS, and 3) they show nonlinear response to PM mass concentration (Charrier et al., 2016; Fang et al., 2016; Calas et al., 2017; Shahpoury et al., 2021). A large number of PM constituents were identified to influence the OP. The DTT assay responds sensitively to ROS produced by organic compounds and indirectly by soluble transition metals, mainly Cu(II), Mn(II) and Fe(II), and can be also influenced by synergetic or antagonistic effects between some chemical components (Charrier and

Anastasio, 2012; Bates et al., 2019; Shahpoury et al., 2021; Borlaza et al., 2022). The AA assay was shown to express large sensitivity to transition metals and some specific organics such as quinones (Künzli et al., 2006; Godri et al., 2011; Visentin et al., 2016).

It is important to extend the studies on this emerging health-related metric to cities and regions in the world. The knowledge on the OP for a large part of Central Europe, namely the Carpathian Basin, is deficient or missing (Szigeti et al., 2015). The major objective of this study was to present, discuss and interpreted the OP data determined by AA and DTT assays in $PM_{2.5}$-fraction aerosol samples collected in parallel in central Budapest, its suburban area and rural background within the Carpathian Basin in each season over one year. We also investigated the spatiotemporal dependencies, and identified the main aerosol sources of OP. The study can contribute to our general knowledge on the OP as well.

2 Methods

2.1 Sample collections

The samplings in the rural background were performed at the K-puszta station (N 46° 57' 56", E 19° 32' 42", 125 m above sea level, a.s.l.), which represents the main plain part of the basin (Salma et al., 2020a). Budapest, with ca. 2.2 million inhabitants in the metropolitan area, is the largest city in the region. Its suburban environment was characterised by collections at the Marczell György Main Observatory (N 47° 25' 46", E 19°10' 54", 138 m a.s.l.) of the Hungarian Meteorological Service (Salma et al., 2022). This is in a southeast residential part of the city. The samplings in the city centre were accomplished at the Budapest platform for Aerosol Research and Training (BpART) Laboratory (N 47° 28' 30", E 19° 03' 45", 115 m a.s.l.), which represents an average atmosphere of the city centre (Salma et al., 2016).

Three identical high-volume sampling devices equipped with $PM_{2.5}$ inlets (DHA-80, Digitel, Switzerland) were deployed at the sites (Salma et al., 2020a). The collection substrates were prebaked quartz fibre filters with a diameter of 150 mm (QR-100, Advantec, Japan). Daily aerosol samples were taken starting at midnight of local time. The samples corresponding to air volumes of 720 m^3 were collected in parallel with each other over semi-consecutive days in October 2017 (autumn), January 2018 (winter), April 2018 (spring) and July 2018 (summer). The total numbers of the filters were 56 in the rural background, 59 in the suburban area, and 28 in the city centre. The samples evenly spread among the four seasons. In addition, one field blank was taken at each location and in each season. The filters were wrapped in preheated Al foils, sealed in plastic bags and stored at a temperature of <–4 °C until the analyses. The

samples represent a gradual transition from the central part of a large continental European city through its suburban area to its regional background in all seasons.

2.2 Analyses and data treatment

Particulate matter mass was determined by gravimetry (Cubis MSA225S-000-DA, Sartorius, Germany, sensitivity of 10 μg). The blank-corrected PM mass data were above the limit of quantitation (LOQ), which was 1 μg m^{-3} (Salma et al., 2022).

Filter punches were analysed by thermal-optical transmission method using a laboratory OC/EC analyser (Sunset Laboratory, USA) adopting the EUSAAR-2 thermal protocol (Cavalli et al., 2010). All blank-corrected organic carbon (OC) and elemental carbon (EC) data were above the LOQ, which were 0.38 and 0.04 μg m^{-3}, respectively. Filter pieces were analysed for levoglucosan (LVG) by gas chromatography–mass spectrometry (Varian 4000, USA) after trimethylsilylation (Blumberger et al., 2019). All blank-corrected LVG data were above the LOQ, which was 1.2 ng m^{-3}.

Parts of the filters were analysed by particle-induced X-ray emission spectrometry for S, Cl, K, Ca, Ti, V, Cr, Mn, Fe, Co, Ni, Cu, Zn, As, Br, Rb, Sr, Zr, Ba and Pb using an external beam of protons with an energy of 2.35 MeV and a current of 20 nA (Aljboor et al., 2022). The obtained spectra were evaluated by the GUPIXWIN program. The filters were treated as thin layer samples. For S, Cl, K, Ca, the self-absorption effects of quartz filters were corrected for (Chiari et al., 2018). The lung bioaccessibility was assessed in the present work by the total amounts of the chemical species as the first approximation.

Concentrations of EC and OC from fossil fuel combustion and from biomass burning (BB), namely EC_{FF} and OC_{FF}, EC_{BB} and OC_{BB}, respectively and of OC from biogenic sources (OC_{BIO}) were previously estimated by a coupled radiocarbon-LVG marker method (Salma et al., 2020a). Secondary organic carbon (SOC) was also assessed previously using the EC tracer method for primary OC (Salma et al., 2022). These results were used as supplementary data in interpretations.

2.3 Determination of oxidative potential

Specified filter areas were extracted in a simulated human respiratory tract lining fluid solution composed of Gamble's solution with dipalmitoylphosphatidylcholine (DPPC; the major phospholipid of lung surfactant; Calas et al., 2017, 2018). The extractions were carried out by vortex agitation at 37 °C for 1 h. The overall procedure represents conditions which are close to the respiratory system. Isoconcentration

extracts with 10 μg ml^{-1} of PM mass were obtained for all samples to overcome possible nonlinear OP response of PM concentrations (Charrier and Anastasio, 2012; Calas et al., 2017).

The sample extracts were not filtered, so they contained insoluble chemical species including those with active surface area (Baumann et al., 2023). The OP was measured by two single-compound in vitro acellular assays, i.e. AA and DTT assays. These two methods are widely used for OP determination (e.g. Calas et al., 2018; Daellenbach et al., 2020; Lionetto et al., 2021; Shahpoury et al., 2021, 2022). However, there is a fundamental difference between them regarding their underlying chemical mechanisms (Charrier and Anastasio, 2012). The quantifications were based on plate-reader spectrophotometry (Tecan Infinite M200 Pro, Switzerland) in MilliQ water for AA, and in a phosphate buffer with a physiological pH value of 7.4 after adding 5,5'-dithiobis(2-nitrobenzoic acid), with readings taken at different specified reaction times (Calas et al., 2018; Borlaza et al., 2021b, 2022). The possible transition metal contamination of the buffer was removed by Chelex 100 resin to reduce the background oxidation. The consumption rates of the AA or DTT were obtained from the simple linear regression of the absorbance values in time at 265 and 412 nm, respectively. The coefficients of determination R^2 for the regression were >0.90 when <70 % of the initial amount of the reagent was oxidised. Matrix absorbance was considered, and the quality assurance of the determinations was performed by positive control tests (Borlaza et al., 2021b). The limits of detection (LODs) for the AA and DTT assays were set at three times the standard deviation (SD) for the blank extracts and were typically 0.008 and 0.0014 nmol min^{-1}, respectively. The experimental protocols were described in more detail previously (Calas et al., 2017, 2018).

The OP data measured by the AA and DTT assays were normalised to $PM_{2.5}$ mass (m) or sampled air volume (V) and are denoted as $OP_{AA,m}$, $OP_{DTT,m}$, $OP_{AA,V}$ and $OP_{DTT,V}$. The consumption rates normalized to V are often considered to have a closer relationship to human exposure, while those normalized by m are regarded as a measure of the inherent OP of PM (Weber et al., 2018; Yu et al., 2019).

2.4 Mathematical models

Source apportionment modelling was accomplished to identify and quantify the main aerosol sources using positive matrix factorisation (PMF, US Environmental Protection Agency, version 5.0; EPA, 2017). It decomposes the sample data matrix into a linear combination of two matrices: a daily factor contribution varying in time and factor profiles by minimizing the critical compound parameter Q (Paatero and Tapper, 1994; Hopke, 2016, 2000). The input data set contained the concentrations and uncertainties of $PM_{2.5}$ mass, S, Cl, K, Ca, Ti, V, Cr, Mn, Fe, Ni, Cu, Zn, Br, Rb, Ba, Pb, EC, OC and LVG for all sampling sites

and seasons. A multisite PMF modelling with 143 samples was performed (Dai et al., 2020). For most chemical species, all concentrations were higher than the LODs. For some trace elements, the concentrations were larger than the LODs in >60 % of the samples. The missing data were replaced by the related median with an uncertainty of 5/6 of the LOD value. The concentrations above LODs were associated with an equation-based extra standard deviation in accordance with the guidelines of the PMF manual, which involved the measurement uncertainty, the concentration and the LOD values (EPA, 2017). Elements Cl, Cr, Ni and Rb were specified as weak variables due to their relatively large SDs.

Several test runs were performed with a total number of factors ranging from 3 to 9 to define the base runs. To explore the goodness of the individual results and to derive robust source apportionment, additional mathematical tools such as bootstrapping and displacement methods were adopted (Norris et al., 2014). In bootstrapping, the compliance between the base factors and bootstrapped factors (which were later selected as the final solution) was >80 %. In addition, the displacement for these solutions did not show larger changes in the parameter Q and no swap counts of factors occurred.

Multiple linear regression (MLR) modelling was performed to deconvolute the measured $OP_{AA,V}$ and $OP_{DTT,V}$ data sets as the dependent variables among the main aerosol sources identified by the PMF as the independent variables (Weber at al., 2021). A linear predictor function was fitted through the dependent variable points by the weighted least squares (WLS) method. The weights were chosen as the inverse of the square of the SD for each measured OP. Goodness of the fit was checked by residual analysis. The significant predictor variables were selected using an *F*-test. The calculations were performed in the advanced analytics software package Statistica (version 7.1, StatSoft, Germany).

3 Results and discussion

3.1 Ranges, averages and tendencies

Basic statistics of the daily OP data and atmospheric concentrations obtained from the filters for the whole sampling interval in the three environments are summarised in Table 1. Some further atmospheric concentrations measured online and the local meteorological data together with their measuring methods are given in Sect. S1 in the Supplement. The concentrations of EC_{FF}, OC_{FF}, EC_{BB}, OC_{BB}, OC_{BIO} and SOC derived earlier can be found in previous publications (Salma et al. 2020a, 2022). The present average concentrations and meteorological data are in line with the results of earlier studies (Salma et al., 2004, 2005, 2020a; Szigeti et al., 2015) suggesting that the overall data set represents typical atmospheric conditions at the locations. However, several Saharan dust intrusions into the Carpathian Basin happened

in April 2018 (Varga, 2020). The most intensive event reached the region via southern Italy and the Balkans on 15 April and affected the studied region for a few days.

Table 1. Ranges and medians of oxidative potential (OP) determined by AA and DTT assays and normalised to PM mass (*m*; $OP_{AA,m}$ and $OP_{DTT,m}$, respectively, in unit of nmol min^{-1} μg^{-1}) or to sampled air volume (*V*; $OP_{AA,V}$ and $OP_{DTT,V}$, respectively, nmol min^{-1} m^{-3}), of concentrations for $PM_{2.5}$ mass (μg m^{-3}), chemical elements (all in ng m^{-3}), elemental carbon (EC), organic carbon (OC, both in μg m^{-3}), levoglucosan (LVG, ng m^{-3}) in the rural background, suburban area and city centre.

Site/ Variable	Rural background			Suburban area			City centre		
	Minimum	Median	Maximum	Minimum	Median	Maximum	Minimum	Median	Maximum
$OP_{AA,m}$	0.01	0.12	0.28	0.02	0.14	0.33	0.03	0.11	0.23
$OP_{AA,V}$	0.1	1.5	5.2	0.3	2.4	11.7	0.3	2.1	4.9
$OP_{DTT,m}$	0.04	0.10	0.20	0.004	0.11	0.27	0.11	0.17	0.27
$OP_{DTT,V}$	0.3	1.2	3.1	0.03	1.9	6.2	1.3	2.9	6.1
$PM_{2.5}$	6	14	29	7	18	46	7	18	44
S	51	311	1043	84	312	823	167	367	952
Cl	5	11	28	5	32	118	5	23	71
K	11	56	234	9	65	363	18	91	264
Ca	1	33	215	6	73	457	23	104	468
Ti	0.05	1.3	15	0.3	1.9	26	0.6	3.1	22
V	0.23	0.46	1.1	0.13	0.43	1.0	0.13	0.44	1.2
Cr	0.16	0.37	0.91	0.18	0.46	1.7	0.17	0.76	7.2
Mn	0.4	2.0	16	0.1	2.1	5.6	0.5	3.3	11
Fe	5	32	162	16	63	306	33	102	607
Ni	0.13	0.42	1.3	0.14	0.33	1.1	0.18	0.57	3.0
Cu	0.13	0.94	6.8	0.6	1.6	7.5	0.8	2.9	27
Zn	0.9	7.2	40	3	12	53	1	17	48
Br	0.20	0.77	3.0	0.2	1.2	4.1	0.5	1.3	2.7
Rb	0.22	0.35	0.76	0.22	0.36	0.83	0.24	0.34	0.80
Ba	1.1	2.4	12	1.1	3.1	12	1.1	4.5	13
Pb	0.6	3.4	28	1.5	5.3	21	1.3	5.6	19
EC	0.08	0.22	0.77	0.21	0.50	1.1	0.31	0.78	1.8
OC	0.9	2.3	6.0	1.0	2.9	11	2.0	3.3	8.0
LVG	4	38	776	5	106	1765	8	203	709

The average $PM_{2.5}$ mass, OP_{AA} and OP_{DTT} data sets showed three different tendencies with respect to the locations. This is better visualised with their annual mean and median data in Fig. 1. The averages (i.e. the medians and means) of the $PM_{2.5}$ mass exhibited a rising trend with levelling off from the rural background through the suburban area to the city centre. The means of both $OP_{AA,m}$ and $OP_{AA,V}$ data sets indicated a maximum in the suburban background, whereas the tendencies for their medians were not fully conclusive. The differences in the tendencies already suggest that there is a misalignment between the PM mass and the OP data and that the two assays used show different sensitivity to source types active at the locations.

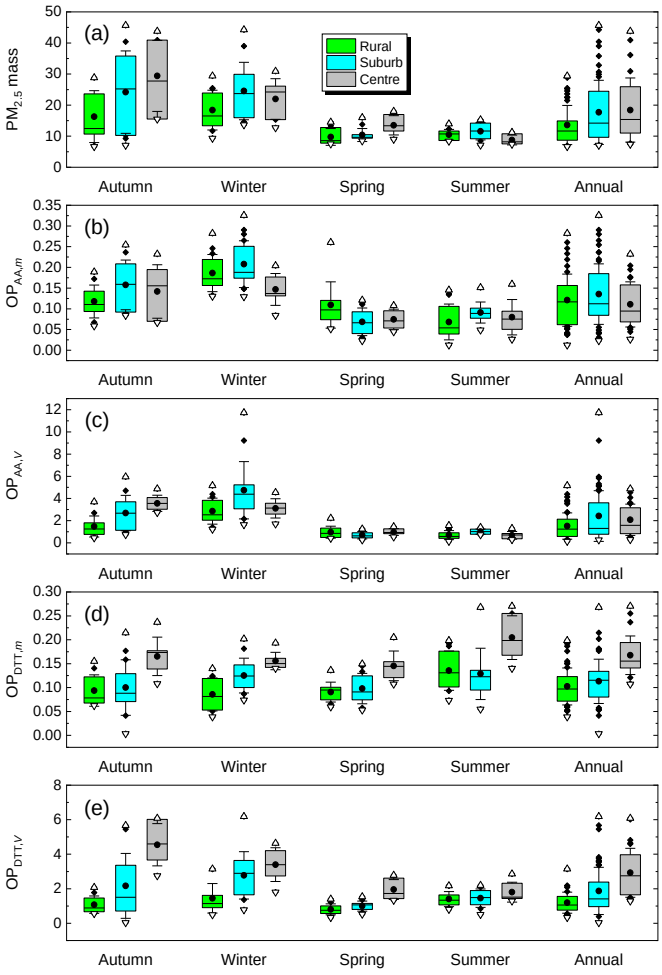

Figure 1. Box and whisker plots of $PM_{2.5}$ mass concentration (µg m^{-3}; panel a), oxidative potential (OP) determined by AA and DTT assays and normalised to PM mass (*m*; $OP_{AA,m}$ and $OP_{DTT,m}$, nmol min^{-1} $µg^{-1}$; panels b and d) or to sampled air volume (*V*; $OP_{AA,V}$ and $OP_{DTT,V}$, nmol min^{-1} m^{-3}; panels c and e) in the rural background, suburban area and city centre separately for each season and over one year. Maximum and minimum values (triangles pointing upward and downward, respectively), further extreme values (diamonds), the first and third quartiles (lower and upper horizontal borders of the boxes, respectively), median (horizontal line inside the boxes), means (bullets) and ±1 SDs (whiskers) of the data sets are shown.

Basic statistics of $PM_{2.5}$ mass and OP data separately for each season and the whole year are shown in Fig. 1. In winter and autumn (the heating period), the OP and PM mass levels were higher than in spring and summer. This is consistent with the other continental European sites (e.g. Calas et al., 2019; Borlaza et al., 2022). The heating period-to-non-heating period OP ratios in the urban locations were larger than for the rural background by factors of ca. 4 for $OP_{AA,V}$ and 1–2 for $OP_{DTT,V}$. There were similar tendencies in the OP values derived by both AA and DTT assays over the seasons. Except for the $OP_{DTT,m}$ data, which showed a fairly constant level over the seasons with some higher values in summer, particularly in

the city centre. This can be again linked to the altered chemical composition of PM mass in time and to the different responses of the two assays to this change.

There are only a few other OP data sets for the $PM_{2.5}$ size fraction derived by AA and DTT assays. Their comparison to our OP data is hindered by important experimental details such as the extracted amount of PM from filters. It can be identified that our median OP values are larger than those at other European sites (Daellenbach et al., 2020; Grange et al., 2022, In 't Veld et al., 2023), while they belong to the middle range of the available results for Japan and China (Kurihara et al., 2022; Yu et al., 2019). The differences can be also influenced by the exact location type since higher OP data near traffic sources were observed (Boogaard et al., 2012; Fang et al., 2016; Daellenbach et al., 2020).

3.2 Consistency between the assays

The dependencies between the OP data derived by the AA assay and normalised either to *m* or *V* on the corresponding DTT data are displayed in Fig. 2. Pearson's coefficients of correlation (*R*) between the data sets normalised to *m* (Fig. 2a) were not significant (p=0.05) at the locations. It suggests that the OP_m was controlled by chemical species that invoked different responses in the assays. However, all correlations between the two OP data sets normalised to *V* (Fig. 2b) were significant. The slopes with SDs of the regression lines were smaller than unity (0.25±0.06, 0.34±0.07 and 0.78±0.13, respectively) and increased monotonically from the rural background through the suburban area to the city centre.

The results suggested that the OP_{DTT} and OP_{AA} values normalised to sampled air volume were in line and consistent. The slopes of their regression lines (Fig. 2b) were <1, which is interpreted as that the AA assay reacted more sensitively to the changes in chemical composition of PM than the DTT assay at our locations. More importantly, the conclusions underline the need for deploying multiple (at least two) OP assays, particularly in cleaner atmospheric environments, to achieve a more holistic and consistent picture (Calas et al., 2017; Bates et al., 2019; Borlaza et al., 2022; Shahpoury et al., 2022).

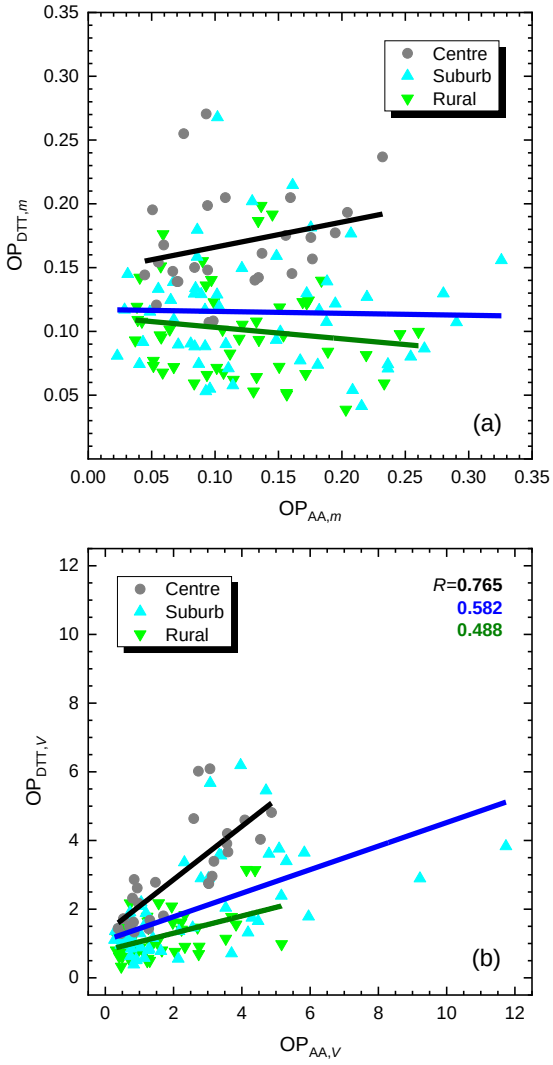

Figure 2. Scatter plots of the oxidative potential (OP) values determined by AA and DTT assays and normalised to PM mass (*m*; $OP_{AA,m}$ and $OP_{DTT,m}$, in nmol min^{-1} μg^{-1}; panel a) or to sampled air volume (*V*; $OP_{AA,V}$ and $OP_{DTT,V}$, nmol min^{-1} m^{-3}; panel b) separately in the rural background, suburban area and city centre. The coefficients of correlation (*R*s) for the significant cases are also given.

3.3 Main aerosol sources

Six factors resolved by the PMF modelling were further evaluated as described in Sect. S2. The following aerosol sources were identified: biomass burning, suspended dust, road traffic, oil combustion mixed with coal combustion and particularly, with long-range transport in the rural background during the nonheating period (Sect. S2), vehicle metal wear and mixed industrial source. Similar set of source types was also identified earlier for Budapest in larger number of samples in winter (Furu et al., 2022).

The apportionments of the $PM_{2.5}$ mass among the main sources are summarised in Fig. 3 separately for each location and season. The plots reveal that the source contributions changed very substantially over the year.

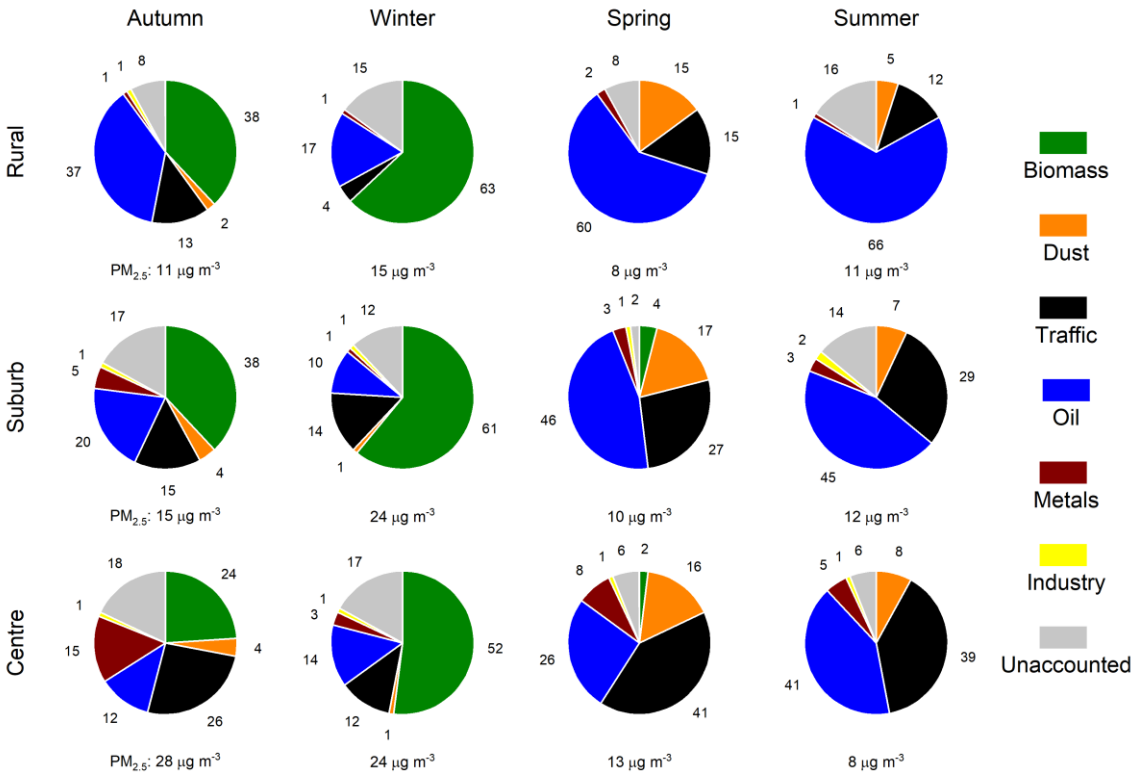

Figure 3. Mean contributions of biomass burning, suspended dust, road traffic, oil combustion mixed with coal combustion and long-range transport, vehicle metal wear, mixed industrial source and unaccounted sources to the atmospheric concentration of $PM_{2.5}$ mass (in %) as derived by the PMF modelling in the rural background, suburban area and city centre in different seasons. The median atmospheric concentrations are shown under the circle charts.

In winter, BB was the dominant source (with mean contributions of 50 % – 60 %) at all sites. In autumn, BB and oil combustion (mixed with coal combustion and long-range transport) were the two most important sources in the rural background with similar shares (38 %). In the suburban area, BB exhibited very similar (38 %) contribution to the rural background, whereas oil combustion and the joint importance of road traffic and vehicle metal wear showed the second largest and similar contributions (20 %). In the city centre, traffic-related sources were the most important contributors (40 %). In spring, oil combustion prevailed (60 %) in the rural background. Its contribution monotonically decreased through the suburban area (46 %) to the city centre (26 %). In parallel with this tendency, the joint share from road traffic and vehicle metal wear increased monotonically (from 17 % through 30 % to 49 %) in the same order of the locations. The contributions from suspended dust in spring were also significant at all locations accounting for approximately 15%. They were influenced by the Saharan dust intrusion episodes extending over the whole Carpathian Basin in this season. In summer, oil combustion was again the dominant source (66 %) in the rural background and showed a decreasing share for the suburban area (45 %) to the city centre (41 %). Contrary, the effects of road traffic monotonically rose (from 13 % through

31 % to 44 %). This increasing tendency was preserved in the other seasons as well. The unaccounted sources and their possible effects on the final results are discussed in Sect. 3.6.

The apportionments of Cu and Fe, which are of special interest for OP, among the main aerosol sources as derived by the PMF modelling are shown in Figs. S7 and S8. Copper mainly or dominantly originated from motor vehicles, i.e. vehicle metal wear and road traffic sources except for the rural background in winter and autumn. The outstanding role of road vehicles is confirmed by our earlier results for a street canyon in central Budapest (Salma and Maenhaut, 2006). The smallest shares from vehicles occurred in winter (22 %, 39 % and 65 %, respectively in the rural background, suburban area and city centre), while the maximum contributions happened in summer (51 %, 65 % and 87 %, respectively). The contribution of unaccounted sources in the rural background in winter was large (33 %), which could modify the apportionments. The role of BB in Cu emissions could be possible explained by illegal industrial and household waste burnings together with biomass (Sect. S2; Hoffer et al., 2021).

In the city centre, the vehicle sources showed the largest contributions to Fe (53 % – 74 %) in all seasons, and dust was its second most intensive source (30 %–36 %) in spring and summer. At the other two locations, Fe in spring was unambiguously dominated by dust (ca. 55 %), which was influenced by the Saharan dust intrusion. Suspended dust remained the most important source in the rural background in summer, whereas it became comparable to the traffic-related sources in the suburban area. Vehicles tended to be the second largest Fe source (26 % – 45 %) in the rural background and suburban area. Their contributions could be partly also associated with the resuspended road dust generated by moving vehicles. In autumn, the shares in the rural background were more or less balanced among the main sources, while the vehicle contributions were increased in the suburban area.

The examples of Cu and Fe demonstrated broadly varying spatial and temporal tendencies in the source contributions of OP-active chemical species and point to the potentials of regulatory measures based on specifically selected source types.

3.4 Oxidative potential and aerosol sources

The OP data normalised to sampled air volume were apportioned to the main aerosol sources, i.e. of BB, suspended dust, road traffic, oil combustion mixed with coal combustion and long-range transport, vehicle metal wear and mixed industrial source using the MLR method with the WLS approach. The slopes and intercepts of the regression lines calculated for the whole data set at each sampling location are summarised in Table S4. In a few cases, negative slopes were obtained. This is commonly found with this

approach, but the absolute values of the negative slopes should be relatively small. This was not the case for the vehicle metal wear and $OP_{DTT,V}$ pair in the rural background, for the road traffic and $OP_{AA,V}$ pair in the suburban area, and for the oil combustion and $OP_{AA,V}$ pair in the city centre. The intercepts of the $OP_{DTT,V}$ in the suburban area and city centre also resulted in statistically nonzero values. These cases jointly indicate that there could be some aerosol sources missing in the PMF modelling due probably to the unavailability of some important marker variables and to the limited number of samples. The shortcoming is further discussed in Sect. 3.6. It cannot be excluded that this imperfection influences the order and mainly the contributions of the OP sources. To improve the attribution of the OP to the identified aerosol sources, the MLR model with the WLS approach was also performed with forced positive slopes option. Its constrained results are summarised in Table 2.

Table 2. Slopes and intercepts of the multiple linear regression with the weighted least squares approach and forced positive slopes option between oxidative potential (OP) determined by AA and DTT assays and normalised to sampled air volume ($OP_{AA,V}$ and $OP_{DTT,V}$, respectively; in nmol min^{-1} m^{-3}) and the main aerosol sources of biomass burning, suspended dust, road traffic, oil combustion mixed with coal combustion and long-range transport, vehicle metal wear and mixed industrial source derived by PMF modelling in the rural background, suburban area and city centre. The number of samples available (*n*) and the adjusted coefficients of determination (R^2) are also shown. Nonsignificant values are in *Italic* font.

Location/	Rural background		Suburban area		City centre	
Main source	$OP_{AA,V}$	$OP_{DTT,V}$	$OP_{AA,V}$	$OP_{DTT,V}$	$OP_{AA,V}$	$OP_{DTT,V}$
Biomass burning	1.414	0.873	0.792	0.622	1.073	0.788
Suspended dust	*0.113*	–	0.569	*0.018*	*0.025*	*0.090*
Road traffic	1.010	0.959	–	*0.181*	0.357	0.887
Oil combustion	0.279	–	*0.522*	0.968	–	*0.488*
Vehicle metal wear	*0.056*	–	–	–	*0.018*	*0.091*
Mixed industrial	–	*0.085*	*0.172*	*0.086*	*0.142*	–
Intercept	*–0.160*	*0.358*	*–0.473*	*–0.497*	*–0.081*	*–0.362*
n	52	51	56	55	28	28
R^2	0.974	0.877	0.717	0.779	0.858	0.811

With this latter option, all intercepts became statistically insignificant ($p<0.05$) from zero. The AA assay yielded significant slopes with BB, road traffic and oil combustion in the rural background, with BB and suspended dust in the suburban area and with BB, and road traffic in the city centre. The DTT assay resulted in significant slopes with BB and road traffic, with BB and oil combustions and with BB and road traffic in the three environments. Comparing the fitted MLR parameters obtained by the constrained and non-constrained WLS approaches (Tables 2 and S4) shows that the orders of the sources did not change substantially, and that the positive slopes obtained by the two models are comparable. At the same

time, the importance of oil combustion decreased in some occasions. These likely indicate that the derived ranks of the OP sources are sensible approximations to reality with some larger uncertainties of their contributions.

The driving effect of BB on OP has been highlighted in other studies (e.g. Verma et al., 2015; Lionetto et al., 2021; Borlaza et al., 2022). The intensity of BB in the Carpathian Basin is, however, large only in the heating period (autumn and winter), and much lower outside this interval. To refine the apportionment of the OP data to aerosol sources active in the non-heating seasons, the MLR modelling was repeated with the joint data set of all sites split into heating and non-heating periods. These results confirmed that BB shows overwhelming contributions to the OP values in the heating period independently of the intensity of the vehicle road traffic. The latter changed substantially among the rural background and urban sites. More importantly, the obtained results also imply that the shares from vehicles (i.e. joint sources of road traffic and vehicle metal wear) to OP prevailed in the non-heating period. This is in line with the attributions of some transition metals such as Cu and Fe to these aerosol sources (Figs. S7–S8 and Salma and Maenhaut, 2006), and also points to the remarkable role of primary traffic emissions in causing oxidative stress in spring and summer.

Secondary organic aerosol under anthropogenically influenced conditions was proven to be one of the top factors for OP (Srivastava et al., 2018; Wong et al., 2019; Daellenbach et al., 2020; Borlaza et al., 2021a, 2021b; Pye et al., 2021; Zhang et al., 2022). The involvement of the SOC concentrations into the PMF was hampered by their smaller count and larger relative uncertainty (up to 30 % – 50 %; Salma et al., 2022). Instead, we investigated the correlations between the OP data sets and SOC concentrations or SOC/OC ratios. The dependencies of the $OP_{DTT,V}$ on the SOC are shown in Fig. S9. The OP values at the urban locations tended to increase with the SOC in parallel with each other, while the OP was rising in a smaller rate in the regional background. The reasons behind these observations likely include the distinct effects of biogenic and anthropogenic secondary organic aerosols typically present in different portions at the sampling locations. The results may indirectly indicate that photochemical aging processes and SOC formation over seasons impact the OP of PM as well (Wong et al., 2019; Kodros et al., 2020; Zhang et al., 2022). The increasing slope of the regression lines from the rural background to the city centre shown in Fig. 2b may also imply that organics of biogenic origin exhibit smaller responses in the DTT assays than those of BB (Verma et al., 2015) or of urban sources in general. There were no significant correlations obtained for the other data pairs.

3.5 Oxidative potential and air quality

Particulate matter mass was proven to be the most important component from the criteria air pollutants in the Carpathian Basin (Salma et al., 2020a, 2020b). Generally, this measure expresses the air quality in the basin. Therefore, the relationships between the $PM_{2.5}$ mass and OP data sets normalised to sampled air volume were separately investigated. Their correlation dependencies were all significant (Fig. 4). Spatial and temporal correlations between these variables from low to moderate were also observed in earlier studies under broadly varying conditions (Künzli et al., 2006; Boogaard et al., 2012; Yang et al., 2015; Fang et al., 2016; Chirizzi et al., 2017).

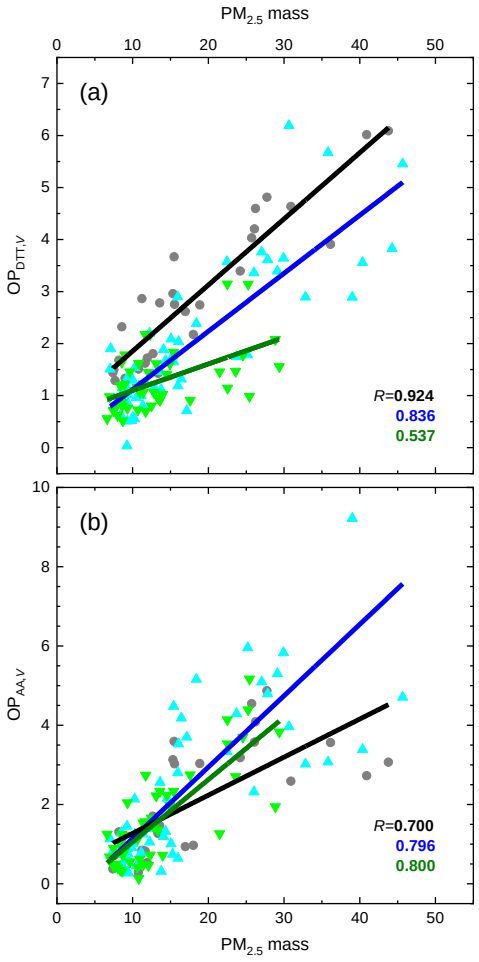

Figure 4. Scatter plots of the oxidative potential (OP) determined by DTT (a) and AA (b) assays and normalised to sampled air volume (V; $OP_{DTT,V}$ and $OP_{AA,V}$, respectively, in nmol min^{-1} m^{-3}) and $PM_{2.5}$ mass concentrations (μg m^{-3}) for the rural background, suburban area and city centre. The lines represent linear regressions of the data sets. The coefficients of correlation (*R*s) are also indicated.

The dependencies for the $OP_{DTT,V}$ (Fig. 4a) resulted in two almost parallel lines (with slopes and SDs of 0.11±0.01 and 0.13±0.01 nmol min^{-1} μg^{-1}, respectively) in the city centre and suburban area, while a

smaller slope (0.051±0.012 nmol min^{-1} μg^{-1}) was observed in the rural background. The situation for the $OP_{AA,V}$ (Fig. 4b) was less obvious but somewhat similar to $OP_{DTT,V}$. The regression lines for the rural background and suburban area tended to be fairly parallel with each other (with slopes and SDs of 0.16±0.02 and 0.18±0.02 nmol min^{-1} μg^{-1}, respectively), whereas the slope for the city centre was smaller (0.096±0.019 nmol min^{-1} μg^{-1}). The intercepts could be typically regarded to be zero within the uncertainty interval.

The parallel tendencies may indicate that the effects of the PM chemical compositions on the given assay were close to each other at the sampling locations with the parallel lines. This was likely caused by spatial and temporal similarities in the main sources such as road traffic and resuspended dust particularly for the DTT assay, and biomass burning especially for the AA assay (Salma et al., 2020a). Particles in the third environment (with the smaller slope) likely contained less OP-active components from the point of the given assay and, therefore, the increase in the OP was more modest. This interpretation is confirmed by earlier similar conclusions (Daellenbach et al., 2020). Nevertheless, it should be stressed that all slopes were substantially and much smaller than unity. This implies that the air quality regulatory measures based on the $PM_{2.5}$ mass are expected to result in smaller improvements in oxidative stress compared to dedicated measures that specifically target (appropriately selected) aerosol sources.

3.6 Limitations and later possibilities

The total numbers of the samples collected at each location represent a limitation mainly for the PMF modelling. To overcome this problem, we applied multisite PMF. It was implicitly assumed in this approach that the main sources active at the locations can be characterised by similar chemical profiles. This is not completely fulfilled for all seasons. An example is the suspended dust which is virtually fugitive mineral and soil dust made of geogenic elements in the rural backgrounds. In the urban sites, it contains further constituents originally generated by anthropogenic activities, which settled down to surfaces and later entered into the air again by resuspension. It is mentioned that the PMF modelling on the separate locations yielded fairly similar results to the multisite approach, while the statistical uncertainties of these latter calculations were favourable.

The unavailability of some secondary inorganics, mainly nitrate and ammonium ions in the present analytical data sets introduced another limitation. Their contributions were likely contained in the unaccounted sources of the PMF modelling. They ranged up to 18 % and showed contributions mainly in colder (heating) seasons or in summer for the rural background and suburban area. Fortunately, pure secondary inorganic constituents are associated with lower contribution to OP of PM (Cassee et al., 2013;

Daellenbach et al., 2020), although they can influence the OP through acid mediated dissolution of transition metals (Fang et al., 2017). However, the robustness of the PMF modelling can influence the final apportion of the OP among the resolved sources.

Larger number of samples and extended list of variables are required because of the basin character of the region of interest. The poorest air quality in the whole Carpathian Basin generally occurs in winter (Salma et al., 2022), when persistent anticyclonic weather situations and lasting temperature inversions happen for longer times. During these intervals, the time series of aerosol constituents, even of different origins, change coherently at many locations due to the common effects of regional meteorology. This dependency can further encumber the separation of the aerosol sources in PMF modelling (Salma et al., 2004).

The present results and conclusions for the OP are strictly valid for the concrete sample preparation and selected assays. A more holistic picture can be achieved by deploying additional and extended experimental methods including those for the sample extraction treatment and OP measurement comprising advantageously both cellular and possibly further acellular assays. The present outcomes can be also improved by involving additional important chemical species and markers, mainly water-soluble metal ions, water-soluble OC, primary biogenic OC and PAHs. Extended research is required to address some additional relevant sources such as coal combustion, biogenic emissions and illegal waste burning. Investigations of size-fractionated aerosol samples with several toxicity indicators and possible synergism or antagonism among chemical species could bring further insights into the oxidative stress research. The experience gained in the present work, which was conducted in a systematic manner for the first time in this region, can form valuable experience in planning further related studies.

4 Conclusions

We showed that the OP induced by $PM_{2.5}$ mass and determined by the AA and DTT assays in the rural (regional) background of the Carpathian Basin, in the suburban area and centre of its largest city of Budapest differed substantially and in a complex manner with location and changed considerably and consistently with season. The alterations were mainly caused by varying intensities of the main aerosol sources and possibly by other specific seasonal features. Biomass burning clearly exhibited the dominant influence at all locations in the heating period. Several pieces of indirect evidence suggest that the joint effects of motor vehicles involving road traffic and vehicle metal wear played the most important role in summer and spring, with considerable contributions from oil combustion and resuspended dust.

The most severe daily PM health limit exceedances in Budapest (and several other European cities) occur in winter due to both residential heating and meteorological effects. The contributions of BB to OP are the largest during this season. Thus, human exposure to high pollution levels is further exacerbated by the chemical composition which causes increased oxidative stress. As far as the sources related to motor vehicles are concerned, large traffic intensities frequently occur in city centres, which generate dangerous hotspots of particularly OP-active species. In these sites, an enhanced exposure of public in summer and spring often coincides with high population densities.

Our conclusions imply that targeting the PM mass in general does not efficiently reduce the oxidative burden from PM exposure. Instead, substantial health improvements could be achieved by focusing on some specific source types such as BB in winter and vehicle traffic in non-heating period. The former source may have timely consequences since it is expected to be increased in the near future. The non-exhaust emissions from vehicle traffic are anticipated to gain in relevance as well since high-efficiency exhaust gas aftertreatment devices had been already adopted to internal combustion engines and because of global spreading of electric vehicles. The advantages of BB and electric cars are often emphasized, while their potential drawbacks have been less disseminated. It is needed to further investigate their distinctive health effects for setting up effective mitigation policies and season-specific regulations.

Data availability. The observational data are available from the corresponding author.

Supplement. The supplement related to this article is available online at: *to be completed*.

Author contributions. MV evaluated the data, performed the modelling calculations, prepared figures, participated in interpreting the results and contributed to writing the manuscript; GU and J-LJ managed the OP measurements, GU, J-LJ and PD participated in interpreting the results and revising the manuscript; ZsK and EP manged the PIXE measurements and participated in interpreting the PMF results; IS conceived the research, arranged the sample collections, evaluated and interpreted the results, prepared figures, wrote the manuscript. All coauthors reviewed and commented on the manuscript.

Competing interests. The authors declare that they have no conflict of interest.

Acknowledgements. The authors are grateful to Anikó Angyal of the Institute for Nuclear Research for the PIXE measurements, to Attila Machon of the Hungarian Meteorological Service for the assistance in the sample collections and the OC/EC measurements, and to Anikó Vasanits of the Eötvös Loránd University for the LVG measurements.

Financial support. This research has been supported by the Hungarian Research, Development and Innovation Office (grants K132254 and K146915), the European Regional Development Fund and the Hungarian Government (grant GINOP-2.3.3-15-2016-00005) and the New National Excellence Program of the Ministry for Innovation and Technology from the source of the Hungarian Research, Development and Innovation Fund (ÚNKP-21-3). The OP analysis was supported by the ACME program (ANR-15-IDEX-02) and ANR Get OP Stand OP program (ANR-19-CE34-0002-01), and were analysed at the Air-O-Sol facility at IGE, made possible with the funding of some laboratory equipment by the Labex OSUG@2020 (ANR10 LABX56).

References

Abrams, J. Y., Weber, R. J., Klein, M., Samat, S. E., Chang, H. H., Strickland, M. J., Verma, V., Fang, T., Bates, J. T., Mulholland, J. A., Russell, A. G., and Tolbert, P. E.: Associations between ambient fine particulate oxidative potential and cardiorespiratory emergency department visits, Environ. Health Perspect., 125, 107008, https://doi.org/10.1289/EHP1545, 2017.

Aljboor, S., Angyal, A., Baranyai, D., Kertész, Zs., Papp, E., Szarka, M., Szikszai, Z., Rajta, I., and Vajda, I.: Light element sensitive in-air millibeam-PIXE setup for fast measurement of atmospheric aerosol samples, J. Anal. At. Spectrom., submitted in 2022.

Apte, J. S., Marshall, J. D., Cohen, A. J., and Brauer, M.: Addressing global mortality from ambient $PM_{2.5}$, Environ. Sci. Technol., 49, 8057–8066, https://doi.org/10.1021/acs.est.5b01236, 2015.

Ayres, J. G., Borm, P., Cassee, F. R., Castranova, V., Donaldson, K., Ghio, A., Harrison, R. M., Hider, R., Kelly, F., Kooter, I. M., Marano, F., Maynard, R. L., Mudway, I., Nel, A., Sioutas, C., Smith, S., Baeza-Squiban, A., Cho, A., Duggan, S., and Froines, J.: Evaluating the toxicity of airborne particulate matter and nanoparticles by measuring oxidative stress potential– a workshop report and consensus statement, Inhal. Toxicol. 20, 75–99, https://doi.org/10.1080/08958370701665517, 2008.

Baumann, K., Wietzoreck, M., Shahpoury, P., Filippi, A., Hildmann, S., Lelieveld, S., Berkemeier, T., Tong, H., and Lammel, G.: Is the oxidative potential of components of fine particulate matter surface-mediated?, Environ. Sci. Pollut. Res., 30, 16749–16755, https://doi.org/10.1007/s11356-022-24897-3, 2023.

Bates, J. T., Weber, R. J., Abrams, J., Verma, V., Fang, T., Klein, M., Strickland, M. J., Sarnat, S. E., Chang, H. H., Mulholland, J. A., Tolbert, P. E., and Russell, A. G.: Reactive oxygen species generation linked to sources of atmospheric particulate matter and cardiorespiratory effects, Environ. Sci. Technol., 49, 13605–13612, https://doi.org/10.1021/acs.est.5b02967, 2015.

Bates, J. T., Fang, T., Verma, V., Zeng, L., Weber, R. J., Tolbert, P. E., Abrams, J. Y., Sarnat, S. E., Klein, M., Mulholland, J. A., and Russell, A. G.: Review of acellular assays of ambient particulate matter oxidative potential: methods and relationships with composition, sources, and health effects, Environ. Sci. Technol., 53, 4003–4019, https://doi.org/10.1021/acs.est.8b03430, 2019.

Blumberger, Z. I., Vasanits-Zsigrai, A., Farkas, G., and Salma, I.: Mass size distribution of major monosaccharide anhydrides and mass contribution of biomass burning, https://doi.org/10.1016/j.atmosres.2019.01.001, Atmos. Res., 220, 1–9, 2019.

Boogaard, H., Janssen, N. A. H., Fischer, P. H., Kos, G. P. A., Weijers, E. P., Cassee, F. R., van der Zee, S. C., de Hartog, J. J., Brunekreef, B., and Hoek G.: Contrasts in oxidative potential and other particulate matter characteristics collected near major streets and background locations, Environ. Health Perspect., 120, 2, https://doi.org/10.1289/ehp.1103667, 2012.

Bondy, S. C.: Anthropogenic pollutants may increase the incidence of neurodegenerative disease in an aging population, Toxicology, 341–343, 41–46, https://doi.org/10.1016/j.tox.2016.01.007, 2016.

Borlaza, L. J. S., Weber, S., Uzu, G., Jacob, V., Cañete, T., Micallef, S., Trébuchon, C., Slama, R., Favez, O., and Jaffrezo, J.-L.: Disparities in particulate matter (PM_{10}) origins and oxidative potential at a city scale (Grenoble, France) – Part 1: Source apportionment at three neighbouring sites, Atmos. Chem. Phys., 21, 5415–5437, https://doi.org/10.5194/acp-21-5415-2021, 2021a.

Borlaza, L. J. S., Weber, S., Jaffrezo, J.-L., Houdier, S., Slama, R., Rieux, C., Albinet, A., Micallef, S., Trébluchon, C., and Uzu, G.: Disparities in particulate matter (PM_{10}) origins and oxidative potential at a city scale (Grenoble, France) – Part 2: Sources of PM_{10} oxidative potential using multiple linear regression analysis and the predictive applicability of multilayer perceptron neural network analysis, Atmos. Chem. Phys., 21, 9719–9739, https://doi.org/10.5194/acp-21-9719-2021, 2021b.

Borlaza, L. J., Weber, S., Marsal, A., Uzu, G., Jacob, V., Besombes, J.-L., Chatain, M., Conil, S., and Jaffrezo, J.-L.: Nine-year trends of PM_{10} sources and oxidative potential in a rural background site in France, Atmos. Chem. Phys., 22, 8701–8723, https://doi.org/10.5194/acp-22-8701-2022, 2022.

Borm, P. J. A., Kelly, F., Künzli, N., Schins, R. P. F., and Donaldson, K.: Oxidant generation by particulate matter: from biologically effective dose to a promising, novel metric, Occup. Environ. Med., 64, 73–74, https://doi.org/10.1136/oem.2006.029090, 2007.

Calas, A., Uzu, G., Martins, J. M. F., Voisin, D., Spadini, L., Lacroix, T., and Jaffrezo, J.-L.: The importance of simulated lung fluid (SLF) extractions for a more relevant evaluation of the oxidative potential of particulate matter, Sci. Rep. 7, 11617, https://doi.org/10.1038/s41598-017-11979-3, 2017.

Calas, A., Uzu, G., Kelly, F. J., Houdier, S., Martins, J. M. F., Thomas, F., Molton, F., Charron, A., Dunster, C., Oliete, A., Jacob, V., Besombes, J.-L., Chevrier, F., and Jaffrezo, J.-L.: Comparison between five acellular oxidative potential measurement assays performed with detailed chemistry on PM_{10} samples from the city of Chamonix (France), Atmos. Chem. Phys., 18, 7863– 7875, https://doi.org/10.5194/acp-18-7863-2018, 2018.

Calas, A., Uzu, G., Besombes, J.-L., Martins, J. M. F., Redaelli, M., Weber, S., Charron, A., Albinet, A., Chevrier, F., Brulfert, G., Mesbah, B., Favez, O., and Jaffrezo, J.-L.: Seasonal variations and chemical predictors of oxidative potential (OP) of particulate matter (PM), for seven urban French sites, Atmosphere, 10, 698, https://doi.org/10.3390/atmos10110698, 2019.

Cassee, F. R., Héroux, M.-E., Gerlofs-Nijland, M. E., and Kelly, F. J.: Particulate matter beyond mass: recent health evidence on the role of fractions, chemical constituents and sources of emission, Inhal. Toxicol., 25, 802–812, https://doi.org/10.3109/08958378.2013.850127, 2013.

Cavalli, F., Viana, M., Yttri, K. E., Genberg, J., and Putaud, J.-P.: Toward a standardised thermal-optical protocol for measuring atmospheric organic and elemental carbon: the EUSAAR protocol, Atmos. Meas. Tech., 3, 79–89, https://doi.org/10.5194/amt-3-79-2010, 2010.

Charrier, J. G. and Anastasio, C.: On dithiothreitol (DTT) as a measure of oxidative potential for ambient particles: evidence for the importance of soluble transition metals, Atmos. Chem. Phys., 12, 9321–9333, https://doi.org/10.5194/acp-12-9321-2012, 2012.

Charrier, J. G., McFall, A. S., Vu, K. K.-T., Baroi, J., Olea, C., Hasson, A., and Anastasio, C.: A Bias in the "Mass-Normalized" DTT Response – An Effect of Non-Linear Concentration-Response Curves for Copper and Manganese, Atmos. Environ., 144, 325–334, https://doi.org/10.1016/j.atmosenv.2016.08.071, 2016.

Chiari, M., Yubero, E., Calzolai, G., Lucarelli, F., Crespo, J., Galindo, N., Nicolás, J. F., Giannoni, M., and Nava, S.: Comparison of PIXE and XRF analysis of airborne particulate matter samples collected on Teflon and quartz fibre filters, Nucl. Instrum. Meth. B, 417, 128–132, https://doi.org/10.1016/j.nimb.2017.07.031, 2018.

Chirizzi, D., Cesari, D., Guascito, M. R., Dinoi, A., Giotta, L., Donateo, A., and Contini, D.: Influence of Saharan dust outbreaks and carbon content on oxidative potential of water-soluble fractions of $PM_{2.5}$ and PM_{10}, Atmos. Environ., 163, 1–8, https://doi.org/10.1016/j.atmosenv.2017.05.021, 2017.

Cho, A. K., Sioutas, C., Miguel, A. H., Kumagai, Y., Schmitz, D. A., Singh, M., Eiguren-Fernandez, A., and Froines, J. R.: Redox activity of airborne particulate matter at different sites in the Los Angeles Basin, Environ. Res., 99, 40–47, https://doi.org/10.1016/j.envres.2005.01.003, 2005.

Cohen, A., Brauer, M., Burnett, R., Anderson, H., Frostad, J., Estep, K., Balakrishnan, K., Brunekreef, B., Dandona, L., Dandona, R., Feigin, V., Freedman, G., Hubbell, B., Jobling, A., Kan, H., Knibbs, L., Liu, Y., Martin, R., Morawska, L., and Forouzanfar, M.: Estimates and 25-year trends of the global burden of disease attributable to ambient air pollution: An analysis of data from the Global Burden of Diseases Study 2015, The Lancet, 389, 1907–1918, https://doi.org/10.1016/S0140-6736(17)30505-6, 2017.

Daellenbach, K. R., Uzu, G., Jiang, J., Cassagnes, L.-E., Leni, Z., Vlachou, A., Stefenelli, G., Canonaco, F., Weber, S., Segers, A., Kuenen, J. J. P., Schaap, M., Favez, O., Albinet, A., Aksoyoglu, S., Dommen, J., Baltensperger, U., Geiser, M., El Haddad, I., Jaffrezo, J.-L., and Prévôt, A. S. H.: Sources of particulate-matter air pollution and its oxidative potential in Europe, Nature, 587, 414–419, https://doi.org/10.1038/s41586-020-2902-8, 2020.

Dhalla, N., Temsah, R. M., and Netticadan, Th.: Role of oxidative stress in cardiovascular diseases, J. Hypertens., 18, https://doi.org/655–673, 10.1097/00004872-200018060-00002, 2000.

Dai, Q., Hopke, Ph. K., Bi, X., and Feng, Y.: Improving apportionment of $PM_{2.5}$ using multisite PMF by constraining G-values with a prioriinformation, Sci. Total Environ., 736, 139657, https://doi.org/10.1016/j.scitotenv.2020.139657, 2020.

Donaldson, K., Tran, L., Jimenez, L., Duffin, R., Newby, D., Mills, N., MacNee, W., and Stone, V.: Combustion-derived nanoparticles: a review of their toxicology following inhalation exposure, Part. Fibre Toxicol., 2, 10, https://doi.org/10.1186/1743-8977-2-10, 2005.

EPA: Positive matrix factorization model for environmental data analyses, https://www.epa.gov/air-research/ positive-matrix-factorization-model-environmental-data-analyses, last access: 20 June 2022, 2017.

Fang, T., Verma, V., Bates, J. T., Abrams, J., Klein, M., Strickland, M. J., Sarnat, S. E., Chang, H. H., Mulholland, J. A., Tolbert, P. E., Russell, A. G., and Weber, R. J.: Oxidative potential of ambient water-soluble $PM_{2.5}$ in the southeastern United States: contrasts in sources and health associations between ascorbic acid (AA) and dithiothreitol (DTT) assays, Atmos. Chem. Phys., 16, 3865–3879, https://doi.org/10.5194/acp-16-3865-2016, 2016.

741 Fang, T., Guo, H., Zeng, L., Verma, V., Nenes, A., and Weber, R. J.: Highly acidic ambient particles, soluble metals, and
742 oxidative potential: a link between sulfate and aerosol toxicity, Environ. Sci. Technol., 51, 2611–2620,
743 https://doi.org/10.1021/acs.est.6b06151, 2017.
744 Furu, E., Angyal, A., Szoboszlai, Z., Papp, E., Török, Z., and Kertész, Z.: Characterization of aerosol pollution in two
745 Hungarian cities in winter 2009–2010, Atmosphere, 13, 554, https://doi.org/10.3390/atmos13040554, 2022.
746 Gao, D., Ripley, S., Weichenthal, S., and Godri Pollitt, K. J.: Ambient particulate matter oxidative potential: chemical
747 determinants, associated health effects, and strategies for risk management, Free Radic. Biol. Med., 151, 7–25,
748 https://doi.org/10.1016/j.freeradbiomed.2020.04.028, 2020.
749 Godri, K. J., Harrison, R. M., Evans, T., Baker, T., Dunster, C., Mudway, I. S., and Kelly, F. J.: Increased oxidative burden
750 associated with traffic component of ambient particulate matter at roadside and urban background schools sites in
751 London, PLoS One, 6, 1–11, https://doi.org/10.1371/journal.pone.0021961, 2011.
752 Grange, S. K., Uzu, G., Weber, S., Jaffrezo, J.-L., and Hueglin, C.: Linking Switzerland's PM_{10} and $PM_{2.5}$ oxidative potential
753 (OP) with emission sources, Atmos. Chem. Phys., 22, 7029–7050, https://doi.org/10.5194/acp-22-7029-2022, 2022.
754 Hoffer, A., Tóth, Á., Jancsek-Turóczi, B., Machon, A., Meiramova, A., Nagy, A., Marmureanu, L., and Gelencsér, A.:
755 Potential new tracers and their mass fraction in the emitted PM_{10} from the burning of household waste in stoves,
756 Atmos. Chem. Phys., 21, 17855–17864, https://doi.org/10.5194/acp-21-17855-2021, 2021.
757 Hopke, P. K.: Review of receptor modeling methods for source apportionment, J. Air. Waste Manag. Assoc., 66, 237–259,
758 https://doi.org/10.1080/10962247.2016.1140693, 2016.
759 Hopke, P. K.: A guide to positive matrix factorization, Clarkson University, Potsdam, USA, 2000.
760 In 't Veld, M., Pandolfi, M., Amato, F., Pérez, N., Reche, C., Dominutti, P., Jaffrezo, J.-L., Alastuey, A., Querol, X., and
761 Uzu, G.: Discovering oxidative potential (OP) drivers of atmospheric PM_{10}, $PM_{2.5}$, and PM_1 simultaneously in North-
762 Eastern Spain, Sci. Total Environ., 857, 159386, https://doi.org/10.1016/j.scitotenv.2022.159386, 2023.
763 Janssen, N. A. H., Yang, A., Strak, M., Steenhof, M., Hellack, B., Gerlofs-Nijland, M. E., Kuhlbusch, T., Kelly, F., Harrison,
764 R., Brunekreef, B., Hoek, G., and Cassee, F.: Oxidative potential of particulate matter collected at sites with different
765 source characteristics, Sci. Total Environ., 472, 572–581, https://doi.org/10.1016/j.scitotenv.2013.11.099, 2014.
766 Katerji, M., Filippova, M., and Duerksen-Hughes, P.: Approaches and methods to measure oxidative stress in clinical
767 samples: research applications in the cancer field, Oxidative Med. Cell. Longev., 12, 1279250,
768 https://doi.org/10.1155/2019/1279250, 2019.
769 Kelly, F. J. and Mudway, I. S.: Protein oxidation at the air-lung interface, Amino Acids, 25, 375–396,
770 https://doi.org/10.1007/s00726-003-0024-x, 2003.
771 Kelly, F. J. and Fussell, J. C.: Size, source and chemical composition as determinants of toxicity attributable to ambient
772 particulate matter, Atmos. Environ., 60, 504–526, https://doi.org/10.1016/j.atmosenv.2012.06.039, 2012.
773 Kelly, F. J. and Fussell, J. C.: Air pollution and public health: emerging hazards and improved understanding of risk,
774 Environ. Geochem. Health, 37, 631–649, https://doi.org/10.1007/s10653-015-9720-1, 2015.
775 Kelly, F. J. and Fussell, J. C.: Toxicity of airborne particles-established evidence, knowledge gaps and emerging areas of
776 importance, Philos. Trans. R. Soc., A378, 2019.0322, https://doi.org/10.1098/rsta.2019.0322, 2020.
777 Kodros, J. K., Papanastasiou, D. K., Paglione, M., Masiol, M., Squizzato, S., Florou, K., Skyllakou, K., Kaltsonoudis, Ch.,
778 Nenes, A., and Pandis, S. N.: Rapid dark aging of biomass burning as an overlooked source of oxidized organic aerosol,
779 Proc. Natl. Acad. Sci. USA, 117, 33028–33033, https://doi.org/10.1073/pnas.2010365117, 2020.
780 Kurihara, K., Iwata, A., Murray Horwitz, S. G., Ogane, K., Sugioka, T., Matsuki, A., and Okuda, T.: Contribution of
781 physical and chemical properties to dithiothreitol-measured oxidative potentials of atmospheric aerosol particles at
782 urban and rural sites in Japan, Atmosphere, 13, 319, https://doi.org/10.3390/atmos13020319, 2022.
783 Künzli, N., Mudway, I. S., Gotschi, T., Shi, T. M., Kelly, F. J., Cook, S., Burney, P., Forsberg, B., Gauderman, J. W.,
784 Hazenkamp, M. E., Heinrich, J., Jarvis, D., Norback, D., Payo-Losa, F., Poli, A., Sunyer, J., and Borm, P. J. A.:
785 Comparison of oxidative properties, light absorbance, and total and elemental mass concentration of ambient $PM_{2.5}$
786 collected at 20 European sites, Environ. Health Perspect., 114, 684–690, https://doi.org/10.1289/ehp.8584, 2006.
787 Lelieveld, J., Evans, J. S., Fnais, M., Giannadaki, D., Pozzer, A.: The contribution of outdoor air pollution sources to
788 premature mortality on a global scale, Nature, 525, 367–371, https://doi.org/10.1038/nature15371, 2015.
789 Lelieveld, J., Pozzer, A., Pöschl, U., Fnais, M., Haines, A., and Münzel, T.: Loss of life expectancy from air pollution
790 compared to other risk factors: a worldwide perspective, Cardiovasc. Res., 116, 1910–1917,
791 https://doi.org/10.1093/cvr/cvaa073, 2020.
792 Lionetto, M. G., Guascito, M. R., Giordano, M. E., Caricato, R., De Bartolomeo, A. R., Romano, M. P., Conte, M., Dinoi,
793 A., and Contini, D.: Oxidative potential, cytotoxicity, and intracellular oxidative stress generating capacity of PM10: a
794 case study in south of Italy, Atmosphere, 12, 464, https://doi.org/10.3390/atmos12040464, 2021.

Norris, G., Duvall, R., Brown, S., and Bai, S.: EPA Positive Matrix Factorization (PMF) 5.0 fundamentals and user guide, Technical Report, U.S. Environmental Protection Agency, National Exposure Research Laboratory, Washington, USA, 2014.

Paatero, P. and Tapper, U.: Positive matrix factorization: A non-negative factor model with optimal utilization of error estimates of data values, Environmetrics, 5, 111–126, https://doi.org/10.1002/env.3170050203, 1994.

Pye, H. O. T., Ward-Caviness, C. K., Murphy, B. N., Appel, K. W., and Seltzer, K. M.: Secondary organic aerosol association with cardiorespiratory disease mortality in the United States, Nat. Commun., 12, 7215, https://doi.org/10.1038/s41467-021-27484-1, 2021.

Riediker, M., Zink, D., Kreyling, W., Oberdörster, G., Elder, A., Graham, U., Lynch, I., Duschl, A., Ichihara, G., Ichihara, S., Kobayashi, T., Hisanaga, N., Umezawa, M., Cheng, T. J, Handy, R., Gulumian, M., Tinkle, S., and Cassee, F.: Particle toxicology and health - where are we?, Part. Fibre Toxicol., 16, 19, https://doi.org/10.1186/s12989-019-0302-8, 2019.

Salma, I., Chi, X., and Maenhaut, W.: Elemental and organic carbon in urban canyon and background environments in Budapest, Hungary, Atmos. Environ., 38, 27–36, https://doi.org/10.1016/j.atmosenv.2003.09.047, 2004.

Salma, I., Ocskay, R., Raes, N., and Maenhaut, W.: Fine structure of mass size distributions in urban environment, Atmos. Environ., 39, 5363–5374, https://doi.org/10.1016/j.atmosenv.2005.05.021, 2005.

Salma, I., Németh, Z., Weidinger, T., Kovács, B., and Kristóf, G.: Measurement, growth types and shrinkage of newly formed aerosol particles at an urban research platform, Atmos. Chem. Phys., 16, 7837–7851, https://doi.org/10.5194/acp-16-7837-2016, 2016.

Salma, I., Vasanits-Zsigrai, A., Machon, A., Varga, T., Major, I., Gergely, V., and Molnár, M.: Fossil fuel combustion, biomass burning and biogenic sources of fine carbonaceous aerosol in the Carpathian Basin, Atmos. Chem. Phys., 20, 4295–4312, https://doi.org/10.5194/acp-20-4295-2020, 2020a.

Salma, I., Vörösmarty, M., Gyöngyösi, A. Z., Thén, W., and Weidinger, T.: What can we learn about urban air quality with regard to the first outbreak of the COVID-19 pandemic? A case study from central Europe, Atmos. Chem. Phys., 20, 15725–15742, https://doi.org/10.5194/acp-20-15725-2020, 2020b.

Salma, I., Varga, P. T., Vasanits, A., Machon, A.: Secondary organic carbon and its contributions in different atmospheric environments of a continental region and seasons, Atmos. Res., 278, 106360, https://doi.org/10.1016/j.atmosres.2022.106360, 2022.

Shahpoury, P., Zhang, Z. W., Arangio, A., Celo, V., Dabek-Zlotorzynska, E., Harner, T., and Nenes, A.: The influence of chemical composition, aerosol acidity, and metal dissolution on the oxidative potential of fine particulate matter and redox potential of the lung lining fluid, Environ. Internat., 148, 106343, https://doi.org/10.1016/j.envint.2020.106343, 2021.

Shahpoury, P., Zhang, Z. W., Filippi, A., Hildmann, S., Lelieveld, S., Mashtakov, B., Patel, B. R., Traub, A., Umbrio, D., Wietzoreck, M., Wilson, J., Berkemeier, T., Celo, V., Dabek-Zlotorzynska, E., Evans, G., Harner, T., Kerman, K., Lammel, G., Noorozifar, M., Pöschl, U., and Tong, H.: Inter-comparison of oxidative potential metrics for airborne particles identifies differences between acellular chemical assays, Atmos. Pollut. Res., 13, 101596, https://doi.org/10.1016/j.apr.2022.101596, 2022.

Srivastava, D., Tomaz, S., Favez, O., Lanzafame, G. M., Golly, B., Besombes, J.-L., Alleman, L. Y., Jaffrezo, J.-L., Jacob, V., Perraudin, E., Villenave, E., and Albinet, A.: Speciation of organic fraction does matter for source apportionment. Part 1: A one-year campaign in Grenoble (France), Sci. Total Environ., 624, 1598–1611, https://doi.org/10.1016/j.scitotenv.2017.12.135, 2018.

Szigeti, T., Óvári, M., Dunster, C., Kelly, F. J., Lucarelli, F., and Záray, G.: Changes in chemical composition and oxidative potential of urban PM(2.5) between 2010 and 2013 in Hungary, Sci. Total Environ., 518–519, 534–544, https://doi.org/10.1016/j.scitotenv.2015.03.025, 2015.

Valavanidis, A., Fiotakis, K., and Vlachogianni, T.: Airborne particulate matter and human health: toxicological assessment and importance of size and composition of particles for oxidative damage and carcinogenic mechanisms, J. Environ. Sci. Health C, 26, 339–362, https://doi.org/10.1080/10590500802494538, 2008.

Valavanidis, A., Vlachogianni, T., Fiotakis, K., and Loridas, S.: Pulmonary oxidative stress, inflammation and cancer: respirable particulate matter, fibrous dusts and ozone as major causes of lung carcinogenesis through reactive oxygen species mechanisms, Int. J. Environ. Res. Public Health, 10, 3886–3907, https://doi.org/10.3390/ijerph10093886, 2013.

Varga, G.: Changing nature of Saharan dust deposition in the Carpathian Basin (Central Europe): 40 years of identified North African dust events (1979–2018), Environ. Int., 139, 105712, https://doi.org/10.1016/j.envint.2020.1057122020, 2020.

Verma, V., Rico-Martinez, R., Kotra, N., King, L., Liu, J., Snell, T. W., and Weber, R. J.: Contribution of water-soluble and insoluble components and their hydrophobic/hydrophilic subfractions to the reactive oxygen species-generating potential of fine ambient aerosols, Environ. Sci. Technol., 46, 11384–11392, https://doi.org/10.1021/es302484r, 2012

Verma, V., Fang, T., Guo, H., King, L., Bates, J. T., Peltier, R. E., Edgerton, E., Russell, A. G., and Weber, R. J.: Reactive oxygen species associated with water-soluble $PM_{2.5}$ in the southeastern United States: spatiotemporal trends and source apportionment, Atmos. Chem. Phys., 14, 12915–12930, https://doi.org/10.5194/acp-14-12915-2014, 2014.

Verma, V., Fang, T., Xu, L., Peltier, R. E., Russell, A. G., Ng, N. L., and Weber, R. J.: Organic aerosols associated with the generation of reactive oxygen species (ROS) by water-soluble $PM_{2.5}$, Environ. Sci. Technol., 49, 4646–4656, https://doi.org/10.1021/es505577w, 2015.

Visentin, M., Pagnoni, A., Sarti, E., and Pietrogrande, M. C.: Urban $PM_{2.5}$ oxidative potential: Importance of chemical species and comparison of two spectrophotometric cell-free assays, Environ. Pollut., 219, 72–79, https://doi.org/10.1016/j.envpol.2016.09.047, 2016.

Wang, S., Ye, J., Soong, R., Wu, B., Yu, L., Simpson, A. J., and Chan, A. W. H.: Relationship between chemical composition and oxidative potential of secondary organic aerosol from polycyclic aromatic hydrocarbons, Atmos. Chem. Phys., 18, 3987–4003, https://doi.org/10.5194/acp-18-3987-2018, 2018.

Weichenthal, S., Shekarrizfard, M., Traub, A., Kulka, R., Al-Rijleh, K., Anowar, S., Evans, G., and Hatzopoulou, M.: Within-city spatial variations in multiple measures of $PM_{2.5}$ oxidative potential in Toronto, Canada, Environ. Sci. Technol., 53, 2799–2810, https://doi.org/10.1021/acs.est.8b05543, 2019.

Weber, S., Uzu, G., Calas, A., Chevrier, F., Besombes, J.-L., Charron, A., Salameh, D., Ježek, I., Močnik, G., and Jaffrezo, J.-L.: An apportionment method for the oxidative potential of atmospheric particulate matter sources: application to a one-year study in Chamonix, France, Atmos. Chem. Phys., 18, 9617–9629, https://doi.org/10.5194/acp-18-9617-2018, 2018.

Weber, S., Uzu, G., Favez, O., Borlaza, L. J. S., Calas, A., Salameh, D., Chevrier, F., Allard, J., Besombes, J.-L., Albinet, A., Pontet, S., Mesbah, B., Gille, G., Zhang, S., Pallares, C., Leoz-Garziandia, E., and Jaffrezo, J.-L.: Source apportionment of atmospheric PM_{10} oxidative potential: synthesis of 15 year-round urban datasets in France, Atmos. Chem. Phys., 21, 11353–11378, https://doi.org/10.5194/acp-21-11353-2021, 2021.

Wong, J. P. S., Tsagkaraki, M., Tsiodra, I., Mihalopoulos, N., Violaki, K., Kanakidou, M., Sciare, J., Nenes, A., and Weber, R. J.: Effects of atmospheric processing on the oxidative potential of biomass burning organic aerosols, Environ. Sci. Technol., 53, 6747–6756, https://doi.org/10.1021/acs.est.9b01034, 2019.

Yang, A., Hellack, B., Leseman, D., Brunekreef, B., Kuhlbusch, T. A., Cassee, F. R., Hoek, G., and Janssen, N. A.: Temporal and spatial variation of the metal-related oxidative potential of $PM_{2.5}$ and its relation to $PM_{2.5}$ mass and elemental composition, Atmos. Environ., 102, 62–69, https://doi.org/10.1016/j.atmosenv.2014.11.053, 2015.

Yu, S., Liu, W., Xu, Y., Yi, K., Zhou, M., Tao, S., and Liu, W.: Characteristics and oxidative potential of atmospheric $PM_{2.5}$ in Beijing: Source apportionment and seasonal variation, Sci. Total Environ., 650, 277–287, https://doi.org/10.1016/j.scitotenv.2018.09.021, 2019.

Yue, Y., Chen, H., Setyan, A., Elser, M., Dietrich, M., Li, J., Zhang, T., Zhang, X., Zheng, Y., Wang, J., and Yao, M.: Size-resolved endotoxin and oxidative potential of ambient particles in Beijing and Zürich, Environ. Sci. Technol., 52, 6816– 6824, https://doi.org/10.1021/acs.est.8b01167, 2018.

Zhang, Z.-H., Hartner, E., Utinger, B., Gfeller, B., Paul, A., Sklorz, M., Czech, H., Yang, B. X., Su, X. Y., Jakobi, G., Orasche, J., Schnelle-Kreis, J., Jeong, S., Gröger, T., Pardo, M., Hohaus, T., Adam, T., Kiendler-Scharr, A., Rudich, Y., Zimmermann, R., and Kalberer, M.: Are reactive oxygen species (ROS) a suitable metric to predict toxicity of carbonaceous aerosol particles?, Atmos. Chem. Phys., 22, 1793–1809, https://doi.org/10.5194/acp-22-1793-2022, 2022.